EMM – An Approach for Prediction of Stability of Rectangular Underground Openings

Anupam Mital*
V.K. Arora

Department of Civil Engineering
National Institute of Technology
Kurukshetra - 136119, India
**Phone: 01744-238497, 238498*

ABSTRACT

In the design of an underground opening, prediction of its stability is the prime objective. After developing suitable equivalent model materials and preparation of models on selection of equivalent material compositions, a systematic study has been carried out using EMM (equivalent material modelling) to study the effect of width of rectangular openings on the deformation of the surrounding rock mass in stratified formation under various overburdens and the effect of height of overburden on stability of openings. Correlations have been developed. A possible solution to intractable problem of ground control has been attempted using in-situ measured data, which can be used for developing design strategies that would minimize ground control hazards, while at the same time maximize recovery at an acceptable cost.

Keywords: Equivalent material modelling (EMM), stability, underground openings, overburden, deformation, limiting span.

1. INTRODUCTION

Construction of hydro-electric, storage, transport and mining projects involve underground openings which often traverse through complex geological formations and varying in-situ conditions. In the design of an underground opening, the prediction of its stability becomes the most important aspect to minimize the chances of failure and consequent possible hazards to personnel and operation while maximizing recovery. Keeping the above facts in view, a laboratory study has been carried out using EMM to study the effect of width of rectangular openings on the deformation of the surrounding rock mass in stratified formations under various overburdens and effect of height of overburden on stability of openings as reported in the paper. The study involved development of equivalent model materials, modelling technique and testing of models.

These studies enabled the investigators to evolve empirical relationships and non-dimensional plots for the evaluation of roof deformations, status of stability and prediction of stable roof spans.

The correlations have been applied to various tunnelling and mining projects. The predicted deformations matched reasonably with the observed deformations. Finally comparison has been made between observed stable roof spans and the predicted stable roof spans using beam theory. The results were found to be in good agreement.

2. EQUIVALENT MATERIAL MODELLING (EMM) TECHNIQUE

EMM is based upon dimensional analysis and similitude. Here, the original rock formations are replaced by artificial materials. Here, the qualitative and quantitative analysis of underground openings can be ascertained. It is one of the best available means for imitating a real specific complex situation. The post -failure behaviour of rock mass surrounding the opening can also be very well ascertained (Bieniawski,1984 and Singh et al.,1985). To evolve an appropriate design approach, one should study the prototype, isolate its constituents and then select parameters relevant to the problem faithfully.

3. DEVELOPMENT OF MODEL MATERIALS AND MODELLING TECHNIQUE

For developing suitable equivalent model materials, 46 mixes of plaster of Paris, fine sand and mica powder were explored. The specimens were tested for compressive strength, tensile strength both along & across the axis and flexural strength after the determination of density. The results of these tests on various EM compositions provided a wide range of equivalent materials (Mittal, 2004).

For developing modelling technique, the physical system selected for simulation and investigations was a Colliery in one of the blocks of Jharia coal field, Jharkhand. Adopting a geometric scale of 1:50, rock mass strength was determined from the sample strength introducing a factor - weakening coefficient of 0.5 from the preliminary model testing. Using Buckingham-Pi dimensional relationships, incorporating weakening coefficient, equivalent strengths were calculated. By finding a suitable matching of the equivalent materials for the required strengths of the formations with due consideration of close proximity of compressive strength and tensile strength, the equivalent formation was designed for the model simulation of the proto formation (Mittal, 2000).

In all, four models of size 3.00 m $\times$ 1.17 m $\times$ 0.25 m were prepared, in layers of 10 mm or 20 mm thickness, in a fabricated frame of size 3.00 m $\times$ 1.80 m $\times$ 0.25 m of mild steel channels. A part of the overburden (38.5 m for models A, B, C & D) was simulated in these models above the proposed opening i.e. roof level. The rest of the overburden upto the ground surface was simulated by applying required surcharge pressures on the top of the models, through a pneumatic loading device in the form of a vulcanised tubular rubber sheet.

4. TESTING OF MODELS

In all, four models were prepared for simulated heights of overburden above the opening of 5600 mm, 4200 mm, 2800 mm and 1400 mm corresponding to their proto values of 280 m, 210 m, 140 m and 70 m respectively.

In these models , 770 mm of equivalent formation corresponding to 38.5 m of proto formation was simulated above the roof of the opening in the form of layers. Therefore, a surcharge pressure equivalent to the overlying mass up to the ground surface was applied on the top of each model. Subsequently, excavation of model was carried out after the necessary instrumentation (Fig. 1).

In between the excavation stages, the duration of the cycle was calculated based on kinematic similarity. This timing was an equivalent cycle of operation corresponding to the normal operational cycle of 3 hours and 30 minutes in the field. This operational cycle of model extraction was calculated using Eq. 1.

$$\frac{T_m}{T_p} = \left(\frac{L_m}{L_p}\right)^{\frac{1}{2}} = (\alpha_L)^{\frac{1}{2}} \qquad (1)$$

where

T_m = cycle of operation in model in minutes,
T_p = cycle of operation of proto in minutes and
α_L = geometrical scale = 0.02 (1:50).

$$\therefore \quad T_m = T_P(\alpha_L)^{\frac{1}{2}} = 210 \times \left(\frac{1}{50}\right)^{\frac{1}{2}} = 29.70 \text{ minutes} \approx 30 \text{ minutes}$$

This operational cycle in model (T_m) was followed for working all the models. The roof deformations were recorded at various monitoring points fixed along rows and columns above the opening. It was observed that the deformations stabilised during this cycle. Here , prominent phenomena were observed visually (Fig. 2).

5. RESULTS AND DISCUSSION

The results obtained from testing of different models are analysed here for the effect of width of opening on roof deformation under different overburdens for prediction of roof deformation and prediction of status of stability of an underground opening.

5.1 Prediction of Roof Deformation

The variation of deformations (Δ_m) at the middle of the opening, just above the roof (20 mm), has been plotted with the width of the opening (w_m) for different heights of overburden (H_m) on a semi-log plot. The variations are shown in Fig.3 for overburden heights of 5600 mm, 4200 mm, 2800 mm and 1400 mm respectively. All these plots

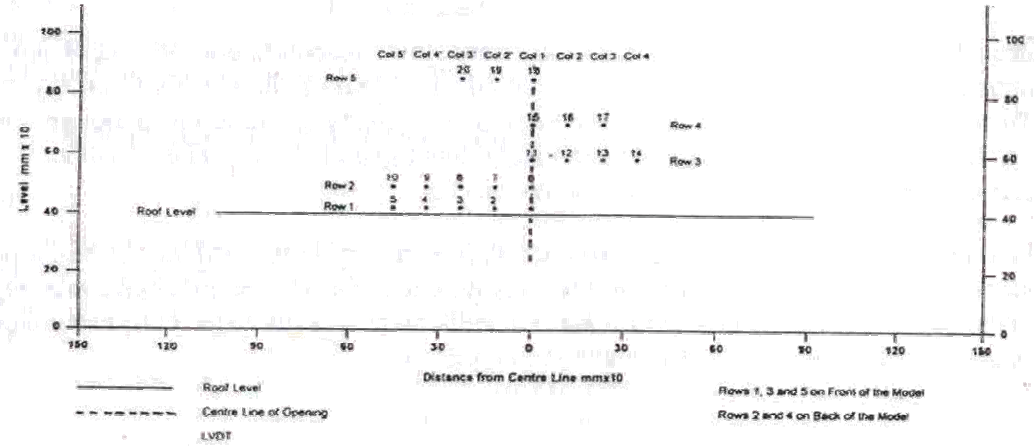

Fig. 1 – Configuration of monitoring points for Model A

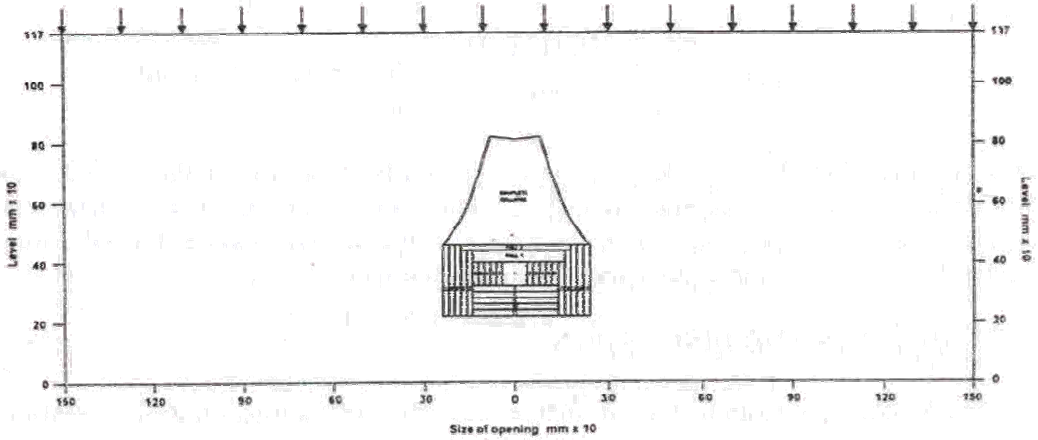

Fig. 2 – Excavation stages and roof falls in Model A

have shown straight line behaviour and therefore, can be expressed in exponential form as

$$\Delta_m = a_m . e^{b_m . w_m} \quad (2)$$

where

Δ_m = deformation of roof of the model in mm,
w_m = width of the opening in model in mm, and
a_m, b_m = constants, whose values are function of overburden pressure $\gamma_m H_m$ in kPa.

(Here γ_m is the unit weight of model material in kN/m^3 and H_m is the height of overburden above the opening in model in m.)

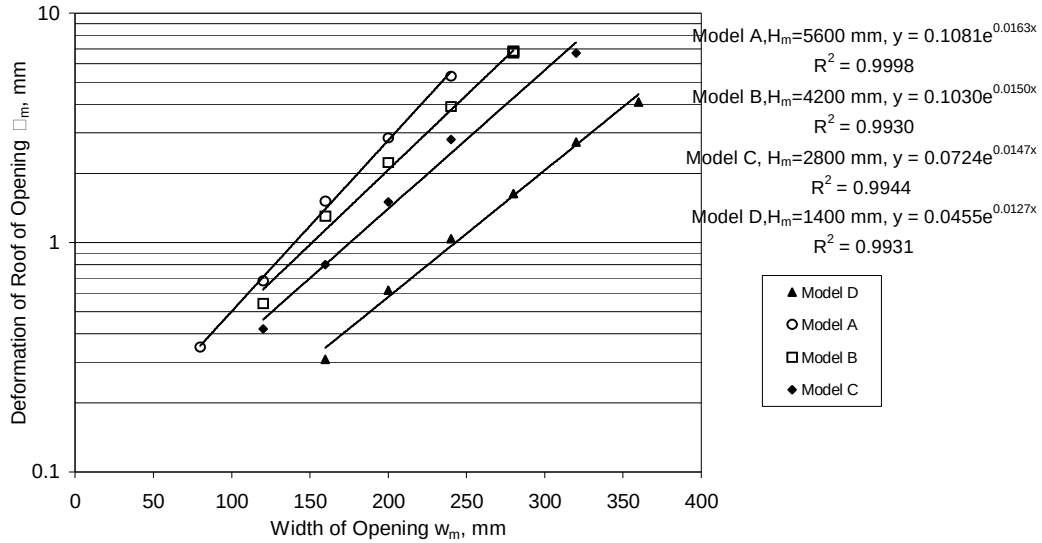

Fig. 3 – Variation of roof deformation with width of opening, Monitoring Point 1

The values of the constants a_m and b_m in Eqn. 2, obtained from the best fit lines of above plots, using method of least squares are as under;

Model	H_m mm	$\gamma_m H_m$ kN/m^2	a_m	b_m
D	1400	14.763	0.0455	0.0127
C	2800	29.526	0.0724	0.0147
B	4200	44.289	0.1030	0.0150
A	5600	59.052	0.1081	0.0163

Seeing the above values, it is observed that the constants a_m and b_m vary linearly with the overburden pressure $\gamma_m H_m$. Their variations are shown in Figs. 4 & 5 in the form of straight lines, whose equations using method of least squares are;

$$a_m = 0.0015\ \gamma_m H_m + 0.0277 \quad (3)$$

with regression coefficient R^2 as 0.9366 and

$$b_m = 8.0 \times 10^{-5}\ \gamma_m H_m + 0.0119 \quad (4)$$

with regression coefficient R^2 as 0.9267.

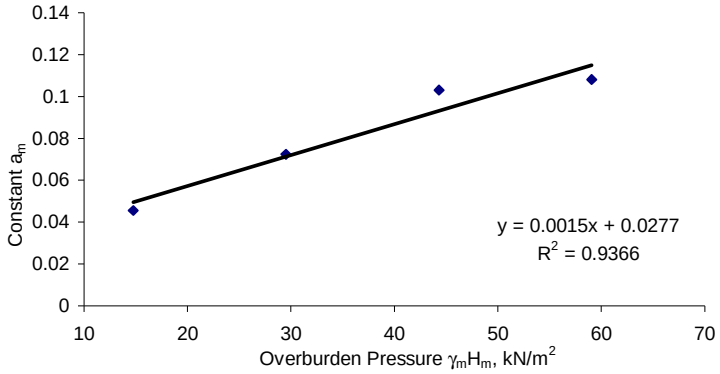

Fig. 4 – Variation of constant a_m with overburden pressure

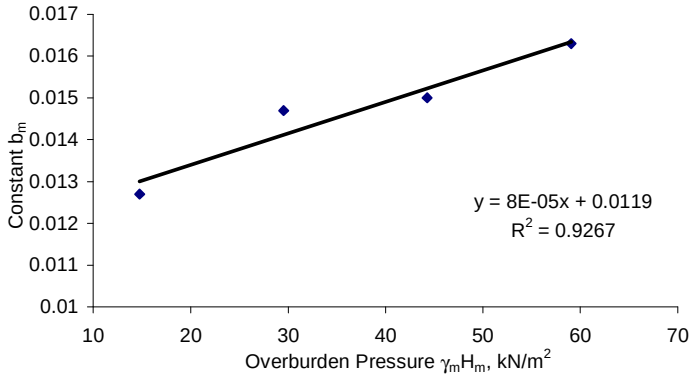

Fig. 5 – Variation of constant b_m with overburden pressure

The complete collapse for the four overburdens had occurred for widths of opening of 600 mm, 520 mm, 500 mm and 480 mm. The deformations corresponding to these widths of opening could not be measured because the LVDTs meant for the same went out of range, due to immediate roof falls. However, the corresponding deformations could be either extrapolated from the plots or calculated using Eqs. 2, 3 and 4.

These equations for model conditions can be used to predict the roof deformation for the proto conditions (Δ_p), using appropriate scale factor in the form ;

$$\Delta_p = a_p . e^{b_p . w_p} \quad (5)$$

where

Δ_p = deformation of roof of the proto in mm,
w_p = width of the opening in proto in mm and
a_p, b_p = constants whose values are function of overburden pressure $\gamma_p H_p$ in kPa.

(Here γ_p is the unit weight of proto material in kN/m^3 and H_p is the height of overburden above the opening in proto in m.)

As constant $a_p = \frac{1}{\alpha_L} . a_m$

Here, $\alpha_L = \frac{1}{50}$,

$\gamma_m = 10.545$ kN/m^3 and

$$\gamma_p = \gamma_{eqp} = \frac{\sum \gamma_{pi} H_{pi}}{\sum H_{pi}} = \frac{g \sum \rho_{pi} H_{pi}}{\sum H_{pi}}$$

$$= \frac{9.807 \times 98157.6}{38.5}$$

$$= 25003.418 \text{ N/m}^3 = 25.003 \text{ kN/m}^3$$

Therefore $\frac{\gamma_m H_m}{\gamma_p H_p} = \frac{10.545}{25.003 \times 50}$

or $\gamma_m H_m = 0.0084 \gamma_p H_p$

Hence, constant $a_p = 50 \times [0.0015 \gamma_m H_m + 0.0277]$

$= 50 \times [0.0015 \times 0.0084 \gamma_p H_p + 0.0277]$

$= 6.3 \times 10^{-4} \gamma_p H_p + 1.385$ (6)

Also, constant $b_p = \alpha_L . b_m$

$$= \frac{1}{50} \times \left[8.0 \times 10^{-5} \gamma_m H_m + 0.0119\right]$$

$$= \frac{1}{50} \times \left[8.0 \times 10^{-5} \times 0.0084 \gamma_p H_p + 0.0119\right]$$

$$= 1.35 \times 10^{-8} \gamma_p H_p + 2.38 \times 10^{-4}$$ (7)

These equations have been applied to various tunnelling and mining projects.

5.2 Prediction of Status of Stability

In order to predict the status of stability of an underground opening, a non-dimensional plot has been proposed, presented in Fig. 6 in terms of deformation of the roof (Δ_p), width of opening (w_p), compressive strength of the immediate roof material

$(\sigma_c)_p$ and overburden pressure (γ_p. H_p) corresponding to two excavation stages with details as under;

For Stage I corresponding to Roof Fall 1,

Model	H_p m	$\gamma_p H_p$ kN/m^2	$(\sigma_c)_p$ kN/m^2	w_p (w_m×50) mm	Δ_p (Δ_m×50) mm	$\frac{(\sigma_c)_p}{\gamma_p H_p}$	$\frac{\Delta_p}{w_p}$	$\left(\frac{\Delta_p}{w_p}\right)^{\frac{1}{2}}$
D	70	1750.21	24941	400×50	365.76	14.25	0.0183	0.135
C	140	3500.42	24941	340×50	536.18	7.13	0.0315	0.178
B	210	5250.63	24941	310×50	625.78	4.75	0.0404	0.200
A	280	7000.84	24941	300×50	718.61	3.56	0.0479	0.219

For Stage II corresponding to Complete Collapse,

Model	H_p m	$\gamma_p H_p$ kN/m^2	$(\sigma_c)_p$ kN/m^2	w_p (w_m×50) mm	Δ_p (Δ_m×50) mm	$\frac{(\sigma_c)_p}{\gamma_p H_p}$	$\frac{\Delta_p}{w_p}$	$\left(\frac{\Delta_p}{w_p}\right)^{\frac{1}{2}}$
D	70	1750.21	24941	600×50	4637.73	14.25	0.1546	0.393
C	140	3500.42	24941	520×50	7558.85	7.13	0.2907	0.539
B	210	5250.63	24941	500×50	9311.42	4.75	0.3725	0.610
A	280	7000.84	24941	480×50	13511.88	3.56	0.5629	0.750

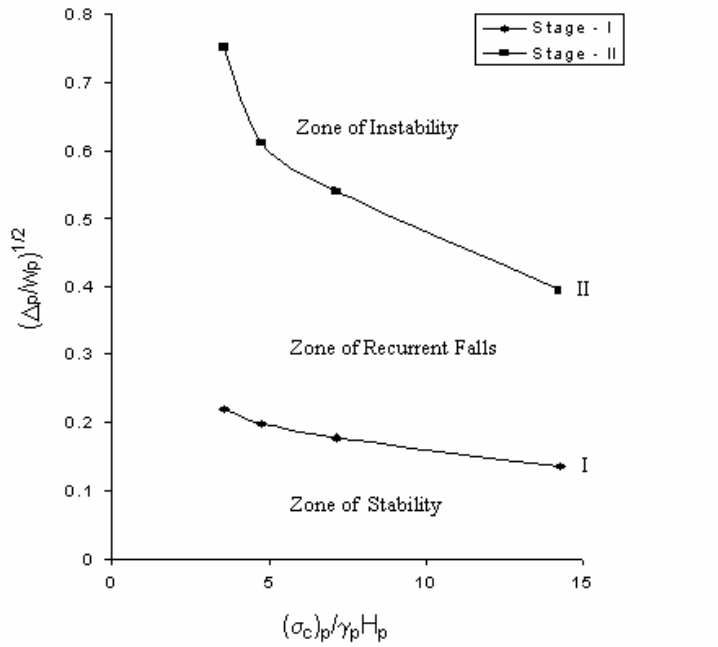

Fig. 6 –Variation of deformation of roof/width of opening with compressive strength/overburden pressure

Curves I and II in Fig. 6 are generated by using predicted deformation values for monitoring point just above the middle of the roof (LVDT No.1) for the two stages I and II. These curves divide the non-dimensional plot area into three zones. The zone located below curve I exhibits 'Zone of Stability'. The zone located in between two curves exhibits 'Zone of Recurrent Falls' and the zone located above curve II exhibits 'Zone of Instability'.

Two other non-dimensional plots proposed on similar lines, exhibiting the three zones are presented in Figs. 4 and 5 where instead of compressive strength of the immediate roof material $(\sigma_c)_p$, flexural strength $(\sigma_f)_p$ and tensile strength $(\sigma_{t2})_p$ have been taken into account, corresponding to the same two excavation stages with details as under ;

For flexural strength,

For Stage I corresponding to Roof Fall 1,

Model	H_p m	$\gamma_p H_p$ kN/m^2	$(\sigma_f)_p$ kN/m^2	w_p (w_m×50) mm	Δ_p (Δ_m×50) mm	$\frac{(\sigma_f)_p}{\gamma_p H_p}$	$\frac{\Delta_p}{w_p}$	$\left(\frac{\Delta_p}{w_p}\right)^{\frac{1}{2}}$
D	70	1750.21	8352	400×50	365.76	4.77	0.0183	0.135
C	140	3500.42	8352	340×50	536.18	2.39	0.0315	0.178
B	210	5250.63	8352	310×50	625.78	1.59	0.0404	0.200
A	280	7000.84	8352	300×50	718.61	1.19	0.0479	0.219

For Stage II Corresponding to Complete Collapse,

Model	H_p m	$\gamma_p H_p$ kN/m^2	$(\sigma_f)_p$ kN/m^2	w_p (w_m×50) mm	Δ_p (Δ_m×50) mm	$\frac{(\sigma_f)_p}{\gamma_p H_p}$	$\frac{\Delta_p}{w_p}$	$\left(\frac{\Delta_p}{w_p}\right)^{\frac{1}{2}}$
D	70	1750.21	8352	600×50	4637.73	4.77	0.1546	0.393
C	140	3500.42	8352	520×50	7558.85	2.39	0.2907	0.539
B	210	5250.63	8352	500×50	9311.42	1.59	0.3725	0.610
A	280	7000.84	8352	480×50	13511.88	1.19	0.5629	0.750

For tensile strength,

For Stage I corresponding to Roof Fall 1,

Model	H_p m	$\gamma_p H_p$ kN/m^2	$(\sigma_{t2})_p$ kN/m^2	w_p (w_m×50) mm	Δ_p (Δ_m×50) mm	$\frac{(\sigma_{t2})_p}{\gamma_p H_p}$	$\frac{\Delta_p}{w_p}$	$\left(\frac{\Delta_p}{w_p}\right)^{\frac{1}{2}}$
D	70	1750.21	659	400×50	365.76	0.3765	0.0183	0.135

C	140	3500.42	659	340×50	536.18	0.1883	0.0315	0.178
B	210	5250.63	659	310×50	625.78	0.1255	0.0404	0.200
A	280	7000.84	659	300×50	718.61	0.0941	0.0479	0.219

For Stage II Corresponding to Complete Collapse,

Model	H_p m	$\gamma_p H_p$ kN/m^2	$(\sigma_{t2})_p$ kN/m^2	w_p (w_m×50) mm	Δ_p (Δ_m×50) mm	$\frac{(\sigma_{t2})_p}{\gamma_p H_p}$	$\frac{\Delta_p}{w_p}$	$\left(\frac{\Delta_p}{w_p}\right)^{\frac{1}{2}}$
D	70	1750.21	659	600×50	4637.73	0.3765	0.1546	0.393
C	140	3500.42	659	520×50	7558.85	0.1883	0.2907	0.539
B	210	5250.63	659	500×50	9311.42	0.1255	0.3725	0.610
A	280	7000.84	659	480×50	13511.88	0.0941	0.5629	0.750

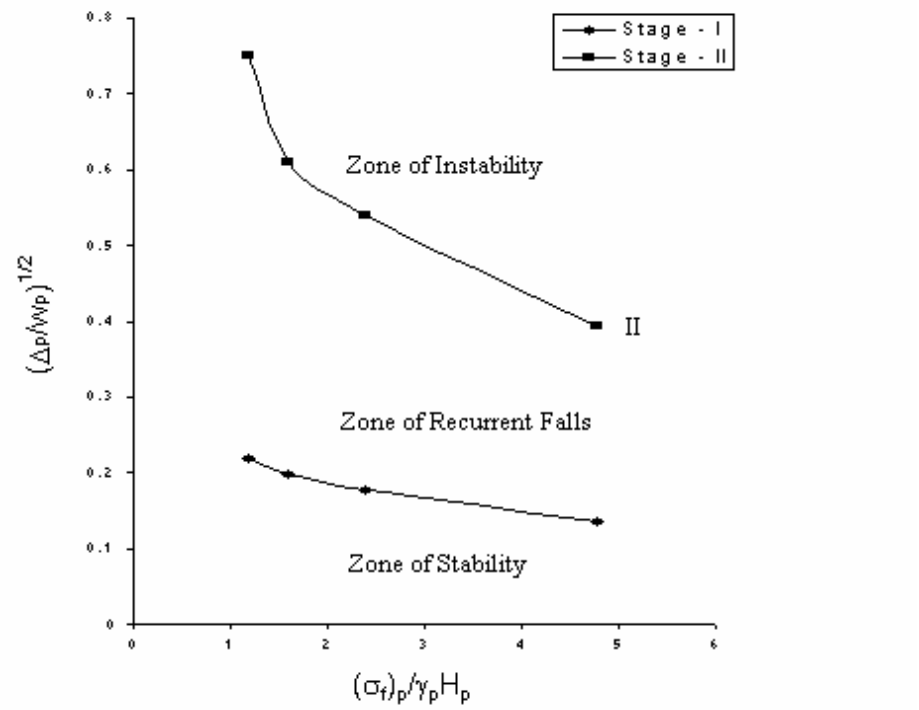

Fig. 7 – Variation of deformation of roof/width of opening with flexural strength/overburden pressure

Further, the most important parameter 'Stable Roof Span' can be predicted using these non-dimensional plots. For a known $\frac{(\sigma_c)_p}{\gamma_p H_p}$ or $\frac{(\sigma_f)_p}{\gamma_p H_p}$ or $\frac{(\sigma_{t2})_p}{\gamma_p H_p}$ ratio, a ratio of stable $\left(\frac{\Delta_p}{w_p}\right)^{\frac{1}{2}}$ can be obtained from Figs. 6 or 7 or 8. From this ratio, Δ_p can be obtained in

terms of w_p, which when substituted in Eq. 5 and using Eqs. 6 and 7 will lead to an optimum value of w_p which will be stable, avoiding premature collapse of the roof and optimising recovery.

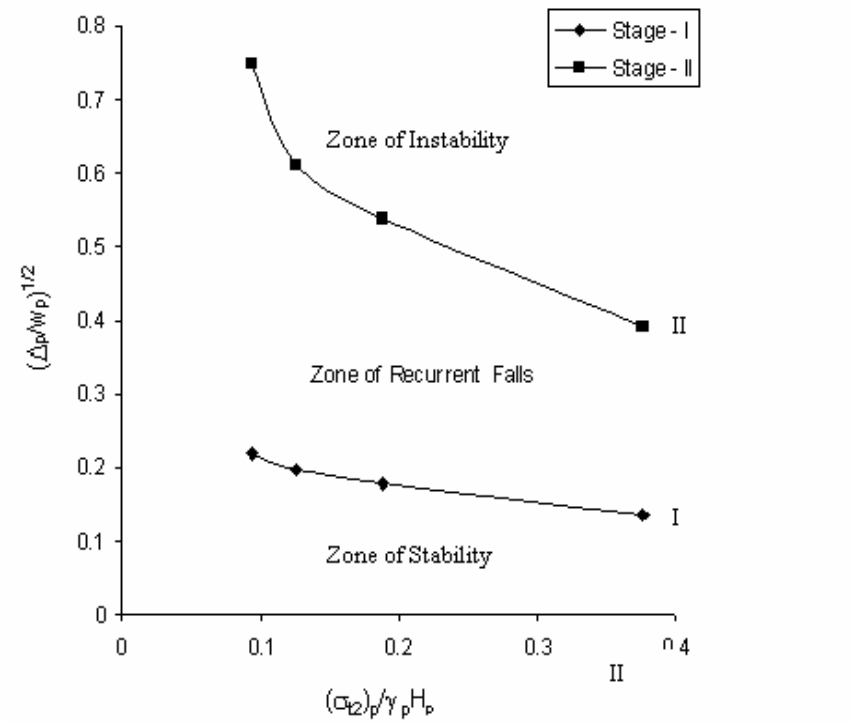

Fig. 8 – Variation of deformation of roof/width of opening with tensile strength (across axis)/overburden pressure

5.3 Comparison of Predicted and Observed Roof Deformations

The observed roof rock mass deformations of four tunnelling and mining projects (Mittal, 2000) are compared with the values predicted from the proposed Eqs. 5 to 7 and the percentage variation is as under;

Name of Project	Observed deformation, mm	Predicted deformation, mm	Variation %
Eisenhower Tunnel	13.00	11.11	14.54
Giri Hydel Tunnel	48.00	33.46	30.21
Satgram Mine	6.68	5.14	23.05
Venkatesh Khani Mine	20.74	16.90	18.51

Though the geological formations of these tunnelling and mining cases are neither exactly stratified nor in the same sequence for which the empirical equations are developed, predicted deformations are still quite satisfactory.

The percentage variation of predicted value from observed value may be attributed to larger time lag in recording the deformation since in the empirical equation proposed, only elastic and plastic deformations, which are independent of time, are considered and time dependent deformations are not taken into consideration.

5.4 Comparison of Predicted and Observed Stable Roof Spans

For the mine under consideration, surface subsidence and sequence of immediate roof falls were the only known features of the mine workings. They offered a narrow scope for the comparison of model and field investigations. The surface subsidence values and the trend of its variation in the mine could not be compared with model studies as a part of the overburden was simulated in the model.

First roof fall in the mine was noted with 16 m face advance when the immediate carbonaceous shale roof came down. Two recurrent falls were observed after 2 and 3 cycles of operation. The complete collapse was noted after 26 m advancement of face. These falls (recurring and complete) were very similar to those of the model observations. In the model C (relevant to the discussion), first fall (Fall 1) was noted after 340 mm face advance (equivalent to 17 m) and the recurring falls of immediate roof were observed after 1 and 3 cycles of operation. The complete collapse was noted after face advance of 520 mm (equivalent to 26 m).

Hence, the sequence of immediate roof falls was observed to be broadly similar to those of the mine workings.

The observed stable roof spans for the four overburdens are compared with the values of predicted roof spans, applying beam theory to the models using equation

$$L = \sqrt{\frac{2\sigma_t Kt}{\gamma}} \qquad (8)$$

The predicted stable roof spans are quite close to their observed values in the models. Equation 8 does not take into account the buckling of layers due to insitu horizontal stresses under high overburden.

Using beam theory for the models D, C, B and A.

Here, σ_t = 21.968 kPa = 21968 Pa = 21968 N/m^2
t = 40 mm = 0.04 m
γ = 771×9.807 N/m^3
K = 0.5

$\therefore$ Limiting span $L = \sqrt{\frac{2 \times 21968 \times 0.5 \times 0.04}{771 \times 9.807}}$

= 0.341 m = 341 mm

The observed stable roof spans for the above four models are compared with the predicted stable roof span using beam theory and the percentage variation is as under;

Model	Overburden kN/m^2	Observed stable roof span, mm	Predicted stable roof span, mm	Variation %
D	14.763	400	341	14.75
C	29.526	340	341	00.29
B	44.289	310	341	10.00
A	59.052	300	341	13.67

Hence, the predicted stable roof spans are quite close to the observed stable roof spans. The decrease in the observed stable roof spans with increase in overburden can be attributed to the fact that a mine roof, even if resolved to an equivalent beam, differs from a fixed-end, self-loaded beam as it always carries a load of the overlying mass until delamination due to differential deflection. By that time, the tensile strength drops to a certain residual value (Singh, 1991).

Hence, the proposed non-dimensional plots may be applied in the field using a safety factor to cover unforeseen geological defects in the roof.

6. CONCLUSIONS

The model studies on underground openings led to development of proper understanding of the ground response above an opening, well in advance, for the formation under consideration. Suitable remedial measures could be adopted in time to safeguard against any expected problem. The developed relationships and suggested zones of stability could be of significant practical utility to the practicing engineers in the stability analysis and optimizing recovery of precious minerals. It is the only available method for observing the progressive failure mechanism (Singh, 1999).

References

Bieniawski, Z.T. (1984). Rock Mechanics Design in Mining and Tunnelling, A.A. Balkema, Rotterdam.

Singh, T.N. and Farmer, I.W .(1985). A Physical Model of an Underground Coal Mine Prototype, Mining Engineering, Vol. 3, pp.319-326.

Singh, T.N.(1991).Underground Winning of Coal, Oxford and IBH, New Delhi, India.

Singh, T.N. (1999). Prediction of Instability of Slope by Equivalent Material Modelling Technique, Proceedings of Workshop on Rock Mechanics & Tunnelling Techniques, Shimla, India, pp.383-390.

Mittal, A. (2000). Model Studies on Underground Openings in Stratified Rocks, *Ph.D.Thesis*, Kurukshetra University, Kurukshetra, India, p. 297.

Mital, A. and Arora, V.K. (2004). Prediction of Stability of Underground Openings Using EMM, Journal of Rock Mechanics and Tunnelling Technology, Vol. 10, No. 2, pp.129-139.